Final Draft
of the original manuscript:

Weigel, T.; Mohr, R.; Lendlein, A.:
Investigation of parameters to achieve temperatures required to initiate the shape-memory effect of magnetic nanocomposites by inductive heating
In: Smart Materials and Structures (2009) IOP

DOI: 10.1088/0964-1726/18/2/025011

Investigation of parameters to accomplish temperatures required to initiate the shape-memory effect of magnetic nanocomposites by inductive heating

Th. Weigel, R. Mohr, A. Lendlein

Center for Biomaterial Development, Institute of Polymer Research, GKSS Research Center Geesthacht GmbH, Kantstr. 55, 14513 Teltow, Germany. Phone +49 3328 352 450; fax +49 3328 352 452; thomas.weigel@gkss.de

Short title

Inductive heating of nanocomposites with shape-memory effect

Key words

Shape-memory polymer, nanocomposite, stimuli-sensitive polymer, AC magnetic field, thermomechanical properties

Abstract

The activation of the shape-memory effect of nanocomposites (NC) by alternating magnetic fields requires exceeding the switching temperature T_s. Different factors, which are influencing this process, have been investigated exemplarily. The intrinsic properties of magnetic nanoparticles (MNP), their content and distribution in the polymer matrix as well as the heat transport conditions, which are essentially determined by the surface to volume ratio (S/V) of the specimens and the surroundings, are influencing the accomplishable temperature in an alternating magnetic field. We used MNP having an iron(II,III)oxide core embedded in amorphous silica, which were homogeneously distributed in a polymer matrix by extrusion molding. The thermoplastic polymer matrix consists either of an aliphatic polyetherurethane (TFX) for demonstration of the basic correlations between magnetic field and the sample, or of a biodegradable multiblock copolymer (PDC), which is prepared from hard segment forming poly(p-dioxanone)diol (PPDO), switching segment forming poly(ε-caprolactone)diol (PCL) and 2,2(4),4-trimethylhexanediisocyanate (TMDI) as junction unit. We could demonstrate that a nanoparticle content up to 10 wt-% do not decisively change the shape-memory properties or mechanical properties of PDC based materials.

1. Introduction

Shape-memory polymers (SMP) belong to the class of active polymers, which are of high scientific and technological significance. They are able to change their shape when exposed to an external stimulus. Most SMP are thermosensitive. The shape-memory effect is not an intrinsic property of a material but a function resulting from a combination of processing

technology and polymer morphology. Initially, the SMP are brought in its original (permanent) shape e.g. by extrusion or injection molding. In an additional programming step, a mechanical deformation of SMP is fixed temporarily (temporary shape). Thermoplastic SMP consist of at least two different phases. The phase with the highest thermal transition (T_{perm}) stabilizes the permanent shape by acting as physical netpoints. The second phase with a lower thermal transition T_{trans} serves as switch. This phase ensures the fixation of temporary shape by crystallization or vitrification by limited flexibility of polymer chains. Heating above T_{trans} can initiate the shape-memory effect because chain segments forming this phase are becoming again flexible and the material shows elastic recovery. T_{trans} can be either glass transition (T_g) or melting temperature (T_m) determined by scanning calorimetry whereas the temperature at which shape-memory effect (T_s) takes place [1] is typically determined by thermomechanical test.

Temperatures exceeding T_s can be realized by increasing the environmental temperature or by heating from the inside by incorporated magnetic particles, which are able to convert the energy of an alternating magnetic field into heat. Only a few papers reported on the magnetic triggering of the shape recovery so far. Particles in the nano- [2] or in the micrometer [3-5] dimension were used, exploiting different physical heating mechanisms, which are based on hysteresis loss and/or related processes that are a direct result of superparamagnetism [6, 7]. Other studies reported inductive heating of smart hydrogels [8], ferrogels [9] and ferrofluids [10, 11] in alternating magnetic fields using embedded magnetic particles.

An essential question is which temperatures for the nanocomposites (NC) can be accomplished by magnetic heating of the nanoparticles, especially for a certain application. In many cases, heat depletion due to convection may be neglected in comparison to heat conduction. In the case of magnetic particle hyperthermia for instance, the heat conduction problem was solved theoretically while assuming a spherical volume filled homogeneously with magnetic particles [12], and proved experimentally too. Limitations in potential temperature are outlined in [13].

SMP have substantial innovation potential in different application areas, e.g. as intelligent implant materials in medicine [14-16]. The combination with non-contact triggering in view of cases where the polymers cannot be warmed up by heat transfer using a hot liquid or gaseous medium will be very promising and calls for more detailed investigations. A successful application of the recently introduced remote triggering of the shape-memory effect by magnetic fields presupposes first of all to obtain the necessary temperature and second the maintenance of the polymer properties even though MNP were incorporated into the polymer matrix.

In the present paper, we evaluate the different possibilities to adjust the temperature, which is necessary for shape recovery by magnetically heating. In order to determine the

temperature, we used an experimental approach in which the conditions preferably are close to potential applications, rather than a theoretical solution of the complex heat transport problem, which would include unavoidably oversimplifications. We do this exemplarily for NC on the basis of established shape-memory polyurethanes. In addition we investigate the dependence of thermal and shape-memory properties on the incorporation of MNP for the biodegradable multiblock copolymer PDC.

2. Materials and Methods

Thermoplastic shape-memory polymers

Cycloaliphatic polyetherurethane Tecoflex® EG72D (TFX) was purchased from Noveon Thermedics Polymer Products, Wilmington, MA, USA. For further information please see Appendix A.

Multiblock copolymer (PDC, for further information please see Appendix B) was synthesized at GKSS according to [15]. The average molecular weight M_w is 292000 g*mol^{-1} and the hard segment content is 50 wt-%.

PPDL-PCL is a multiblock copolymer similar to PDC with a hard segment of poly(pentadecalactone) and was also synthesized at GKSS.

Desmopan and Elastollan are commercially available polyurethanes, provided by Bayer and BASF, respectively.

Nanoparticles

Nanoscaled particles AdNano® MagSilica 50, 50-H8 and 50-85 were provided by Degussa Advanced Nanomaterials, Degussa AG, Hanau, Germany [17]. For further information please see Appendix C.

Preparation of polymer composites

TFX - Composites

Compounding of MNP was carried out with a co-rotating twin screw extruder HAAKE PolyLab System PTW 16/25 (Thermo Electron Corp., Waltham, USA). The processing temperature was in the range between 165 and 170 °C. Prior to the processing, the materials were milled, mixed, and dried in a vacuum oven at 65 °C for 4 h. Extrusion was performed at screw speeds 100 and 150 rpm [2].

PDC - Composites

PDC based compounds were performed in a small conical counter rotating twin screw extruder HAAKE PolyLab Rheomex CTW5 (Thermo Electron Corp. Waltham, USA). PDC was gravimetrically mixed with the MNP before extrusion. Processing temperature was 120 °C, screw speed 150 rpm.

Morphology characterization

Particle distribution was determined by scanning electron microscopy (SEM) in backscattering mode with a Zeiss Supra 40 VP (Carl Zeiss, Oberkochen, Germany).

Differential scanning calorimetry (DSC)

DSC experiments were performed on a Netzsch DSC 204 (Netzsch GmbH, Selb, Germany) in the temperature rage from -80 °C to 150 °C. For further information please see Appendix D.

Thermogravimetry (TGA)

The nanoparticle content within the NC was determined by completely combustion in a N_2/O_2 atmosphere up to 900 °C.

Dynamic mechanical analysis at varied temperature (DMTA)

The determination of the dynamic mechanical properties was performed on a Gabo Eplexor® 25 N (Gabo GmbH, Ahlden, Germany) in the temperature range from -100 °C to 100 °C. For further information please see Appendix E.

Magnetic field application

Heating is realized by positioning the sample in an alternating magnetic field at frequencies between f = 253 and 732 kHz. While the frequency could only be varied in defined intervals, the experimental setup allows the infinitely variable magnetic field strength in the center of the coil between 7 and 30 $kA \cdot m^{-1}$ by adjusting the power output of the generator. For details about the determination of the magnetic field strength, see [2].

The equipment consists of high-frequency generators TIG 5/300 and Axio (both Huettinger Elektronik GmbH&Co. KG, Germany) and water-cooled coils with diameters of 4 and 5 cm as well as lengths of 6 and 12 cm, respectively. The coils had 6 and 10 windings, respectively.

Temperature measurement

An IR - Pyrometer Metis My84 from Sensortherm GmbH, Germany, was used for non-contact measuring of the sample temperature. The direct temperature measurement was carried out by self-made Cu-CuNi thermocouples which were included into the sample.

The magnetically relevant system was located within an incubator that could control the temperature between ambient +3 °C and 60 °C.

Tensile tests and cyclic thermomechanical experiments

Tensile and thermomechanical tests were performed on Zwick Z1.0 and Z005 tensile testers equipped with thermo chambers (Zwick, Ulm, Germany) and temperature controller (Eurotherm Regler GmbH, Limburg, Germany). The strain rate was 5 $mm \cdot min^{-1}$ in all experiments.

Test specimens for mechanical characterization were processed on a polymer press type 200 E (Dr. Collin GmbH, Ebersberg, Germany). Processing parameters for the PDC materials are 100 °C, 100 bar for 5 min. Typically the film thickness was 0.3 mm for the

cyclic, thermomechanical experiments. Specimens according to DIN EN ISO1BB [18] were cut with a punching tool, l_o = 20 mm, width 2 mm (Figure 1).

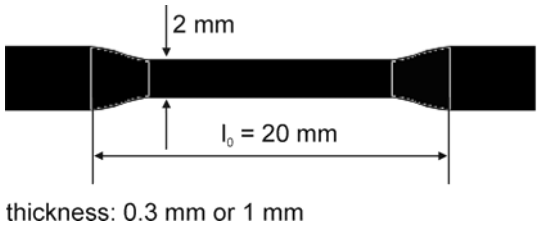

Figure 1: Shape of test specimens for thermomechanical experiments.

Test specimens with a thickness of 1 mm for temperature measurement in the magnetic field were obtained by injection molding at 120 °C (PDC) and 140 °C (TFX).

Programming of PDC materials for cyclic thermomechanical tensile tests

In a first step the sample is deformed to ε_m = 150% at T_{high} = 55 °C (warm programming) or T_{deform} = 25 °C (cold drawing). After keeping this deformation for 5 minutes to allow relaxation, the stress is held constant while the sample is cooled to T_{low} = 0 °C whereby the temporary shape is fixed. Then stress is lowered to zero. The sample now is in its temporary shape. Finally, the sample is warmed up to T_{high} = 65 °C with a heating rate of 2 K·min^{-1}. After waiting for 10 min, the next cycle is performed.

3. Results and Discussion

A remote triggering of the shape-memory effect of polymeric nanocomposites via an alternating magnetic field requires the realization of a series of conditions, which are the parameters of the magnetic field (frequency and field strength), the particle content within the polymer matrix, the specific absorption rate of magnetic particles, the particle distribution and polymer matrix, the sample geometry and the surrounding of the sample. Only an optimal linking of all these interdependent conditions enables the achievement of a temperature which is sufficient for triggering the shape-memory effect.

Specific absorption rate

We prepared NC with different polymer matrices and MNP which were based on iron oxide in a silica shell. Since it is well known that all MNP differ in their loss powers due to structural magnetic particle properties and dimensions [7], we have investigated the specific absorption rate (SAR) of the MagSilica powders with the help of a calorimetric method that measures the initial temperature increase dT/dt of nanocomposites in the first 10 seconds with the IR - pyrometer. Calorimetric measurement of SAR is a standard method as described in [11, 19]. SAR, which is often also called specific loss power, is then calculated according to (1), $y_{MagSilica}$ is the nanoparticle portion, $c_{p,comp}$ is the specific heat capacity of the nanocomposite, which was determined to 1.7 J/Kg independently on the content of MNP via DSC. The dependence of the specific heat capacity on the temperature was neglected.

$$SAR = c_{p,comp} \frac{dT}{dt} \frac{1}{y_{MagSilica}} \quad (1)$$

The observed SAR corresponds well in magnitude with literature data regarding iron oxide nanoparticles [9, 11, 19-25] and shows a dependence on the magnetic field strength to the power of 2.5 (Figure 2). In this diagram SAR references directly to the content of iron oxide in the MNP. Both the obtained dependence on magnetic field strength and the obtained linear dependence on frequency (Figure 3), are an evidence, that the present particles are in the transition region between losses due to superparamagnetism and hysteresis [26, 27]. Because of the power dependence on the magnetic field strength in comparison to the linear one on frequency, increase of field strength should be preferred in order to enhance the heat production. Regarding to iron oxide all three types of AdNanoMagSilica are equivalent, but MagSilica 50-85 powder causes the highest temperature increase at equal portions in the matrix due to the highest fraction of iron oxide.

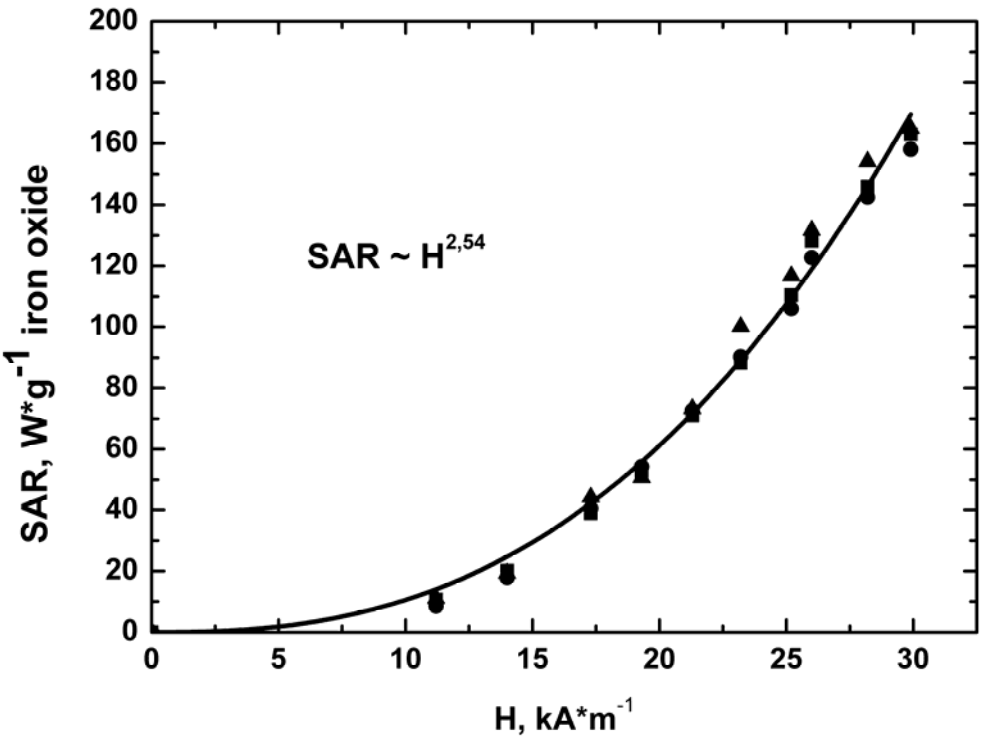

Figure 2: Specific absorption rate (SAR) of different nanoparticles in dependence on magnetic field strength H (■ MagSilica 50, ● MagSilica 50-85, ▲ MagSilica 50-H8; f = 254 kHz).

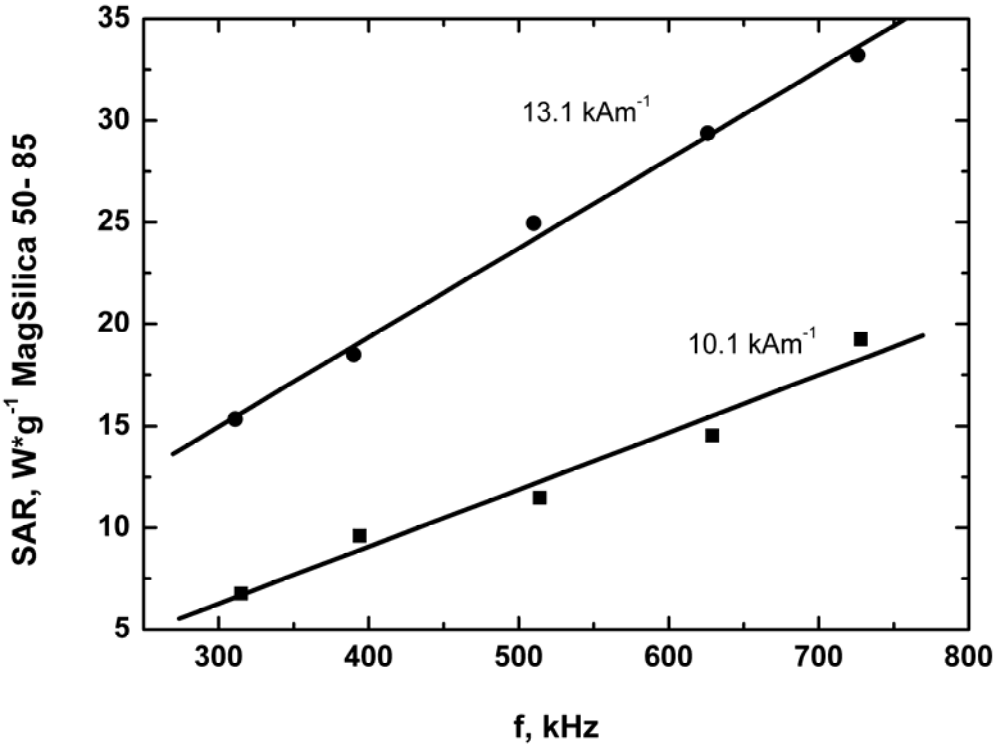

Figure 3: Specific absorption rate (SAR) of nanoparticle AdNanoMagSilica 50-85 (TFX 144) depending on frequency of the magnetic field strength H.

Particle distribution and content

A homogeneous distribution of the MNP, which is a prerequisite for a consistent heating of the nanocomposite, has been obtained by extrusion molding (Figures 4a, b, c). A few agglomerated particles in the range of microns are already existent in the initial nanopowder as SEM investigations revealed.

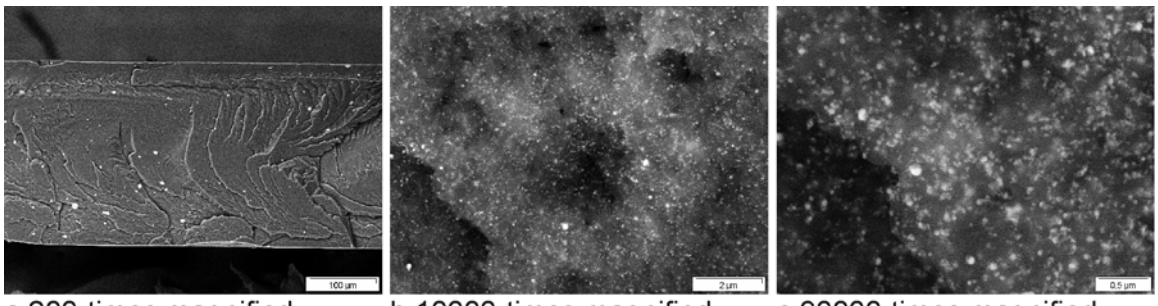

a 200-times magnified b 10000-times magnified c 30000-times magnified

Figure 4: SEM pictures, 10 wt-% nanoparticles AdNanoMagSilica 50 in TFX.

Increasing the particle content and the magnetic field strength is leading to higher temperatures (Figure 5).

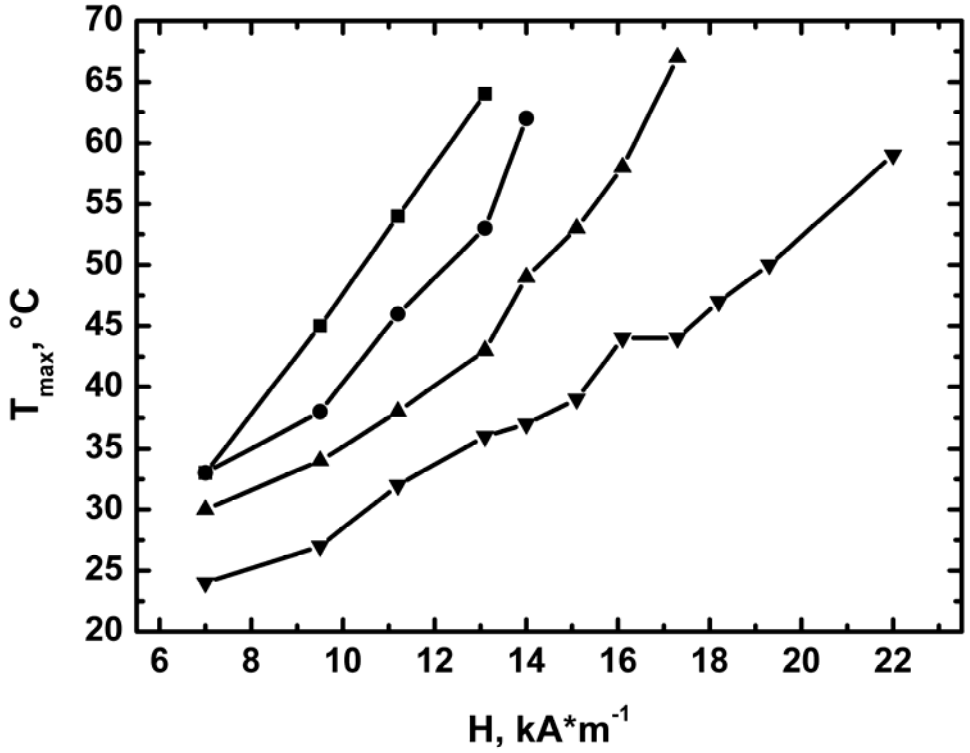

Figure 5: Temperatures achieved for TFX composite samples (injection molded) when exposed to a magnetic field (f = 255 kHz), TFX200 = 20 wt-% nanoparticles (-■- TFX200, -●- TFX150, -▲- TFX100, -▼- TFX050).

Polymer matrix

Because of very similar heat properties of all thermoplastic polymers, there was no remarkable influence on heating in the magnetic field (Figure 6). All used polymers have shape-memory properties.

Because of the similar heat properties of different polymers, it is justified to perform basic investigations with an established shape-memory polyurethane (Tecoflex), the results are transferable to biodegradable NC, for instance the multiblock copolymer PDC.

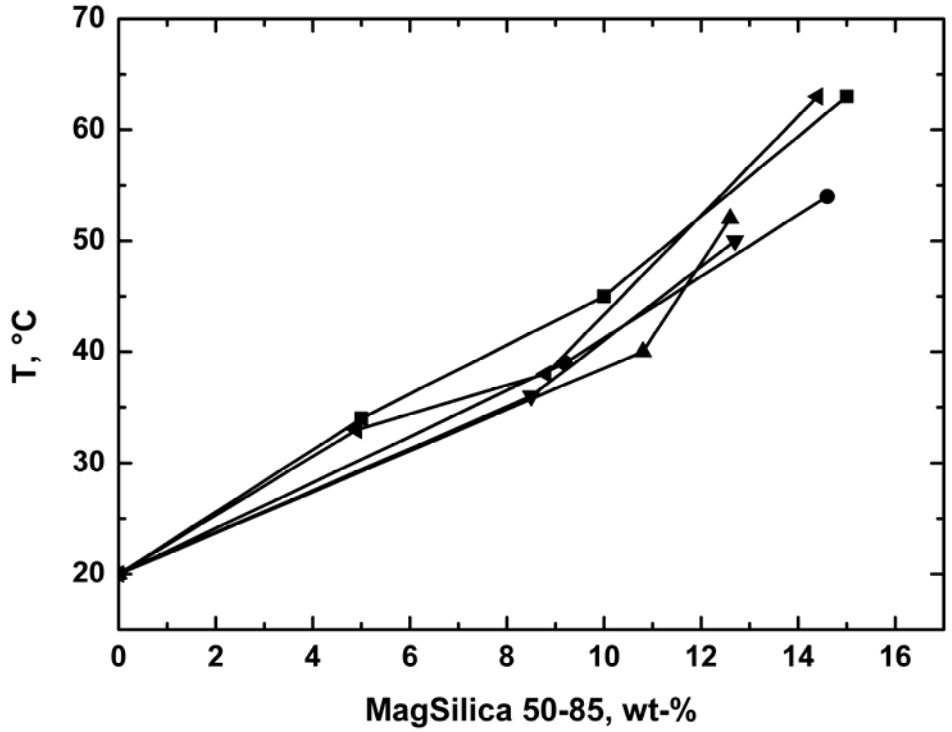

Figure 6: Temperatures achieved for nanocomposites (injection molded sample, thickness = 1 mm) with different polymeric matrices (-■- PPDL-PCL, -●- Desmopan W, -▲- Desmopan 385, -▼- Elastolan, -◀- Tecoflex EG 72) when exposed to a magnetic field (f = 254 kHz, 11.2 $kA*m^{-1}$).

Sample geometry

According to the laws of heat conduction, the sample's surface to volume ratio (S/V) is one of the most important criterions concerning the heating of NC in a magnetic field. The higher the S/V the lower the accomplishable temperature difference (Figure 7). At an S/V difference of one magnitude the difference in temperature is after all about 30 °C for the selected example. This has to be kept in mind for application purposes.

Closely related to the heat transfer via the surface is the nature of the surrounding. All experimental data reported so far were obtained in air.

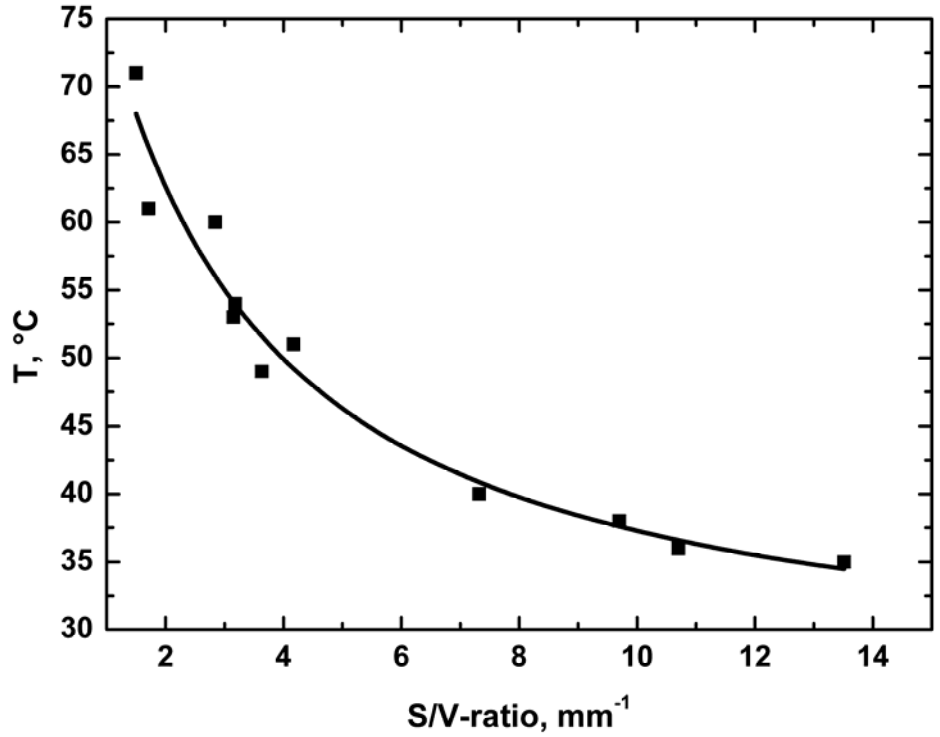

Figure 7: Temperatures (starting from room temperature) achieved for nanocomposites (TFX075) with different surface to volume ratio (S/V) when exposed to a magnetic field (f = 253 kHz, 14 kA*m^{-1}).

Nature of Environment

For medical application for instance, we have to consider that the environment is typically aqueous, and it is well known that water is a much better cooling medium than air because of its higher heat conductivity (25 times higher than air) and much higher heat capacity per volume. Therefore the heat-transfer coefficient of the composite at the interface to water is for magnitudes greater than to air, and it is more difficult to reach T_s in the composite.

Hence, the experimentally accomplishable temperatures for identical samples achieve in water approximately only one third from the magnitude in air (Figure 8). The environmental temperature was in this experiment 29 °C. In the case of heating in air by switching-on the magnetic field, the sample temperature is immediately increasing and reaching a plateau. Because of the restricted volume (15 ml) of water or gelatine solution in the experimental setup, the temperature here is afterwards slightly increasing with time due to warming up of the surrounding. Switch-off of the magnetic field causes a sudden temperature decrease, which is naturally more accentuated in the case of air.

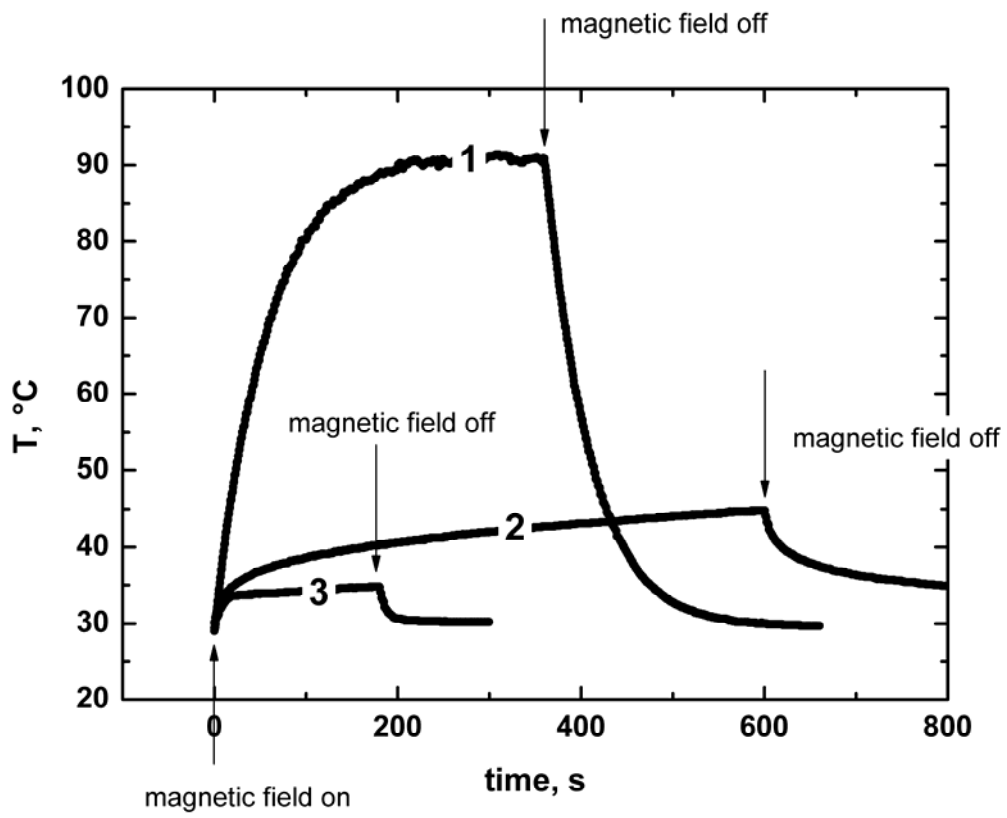

Figure 8: Heating curves for a nanocomposite (18.1 % MagSilica 50 in TFX - TFX181) in different surroundings of 29 °C, 1 - air, 2 - 10 % gelatine in 0.5 % NaCl solution, 3 - distilled water (f = 254 kHz, H = 11.2 kA*m^{-1}).

With regard to a potential application of biodegradable NC within the human body for instance as suture, we tested the temperatures that could be accomplished in meat. NC samples with 14.4 wt-% MagSilica 50 and different S/V were embedded in meat of pork with a temperature of 37 °C and heated at different magnetic field strengths. As expected, the temperatures were higher in comparison to those one could accomplish in water. Figure 9 shows the temperature-time-plots for a sample with a surface to volume ratio of 8.3. At magnetic field parameters of 14 kA*m^{-1} and 253 kHz temperatures up to 42 °C depending on time could be accomplished. The chosen field parameters were in the region that is classified as compatible for human beings [28, 29]. Having in mind T_s of PDC based nanocomposites are between 40 and 45 °C [15], an application of NC based on this biodegradable polymer for magnetically heating is difficult to realize and requires optimization of all the influencing parameters.

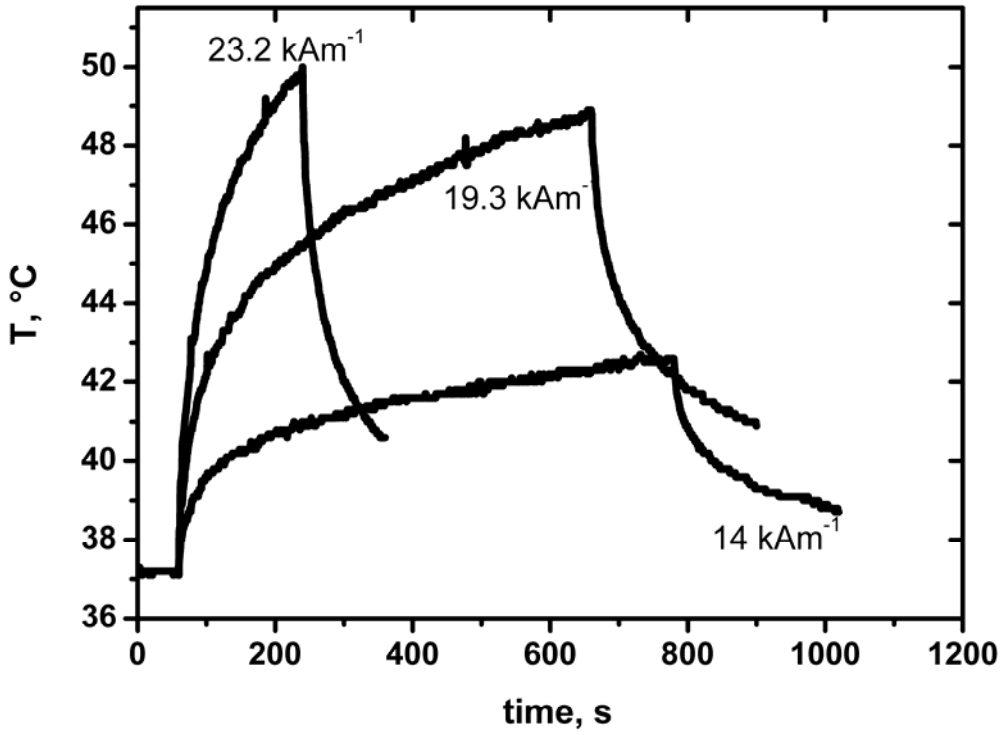

Figure 9: Heating curves for a nanocomposite (14.4 wt-% MagSilica 50 in TFX – TFX144) with a S/V = 8.3 in meat (from pork) at different magnetic field strengths (f = 254 kHz, starting from 37 °C).

The recovery of deformed NC of PDC in the magnetic field is described in [2]. If T_s is exceeded, the shape recovery occurs just as well as by heating the environment. It is irrelevant whether the heat comes from inside or outside. Simply the heating rate, which could vary, may causes differences in the velocity of shape recovery, but these phenomena are not the subject of our present investigation. We focused on the influence of incorporated MNP on thermal, mechanical and shape-memory properties of PDC nanocomposites. Thereby we have been concentrated on AdNanoMagSilica 50-H8 with a hydrophobic coating, because only the NC with these particles enabled warm and cold programming (Table 1a). The elongation at break at 55 °C for NC with AdNanoMagSilica 50-85 particles was too small for performing the warm-programming with elongations of 150% (Table 1b).

Table 1: Mechanical properties of PDC nanocomposites, E is the elastic modulus, σ_b is the stress at break, and ε_b is the elongation at break, E'_c/E'_r is the ratio of storage modulus at 25 and 55 °C, obtained from DMTA

a) MagSilica 50-H8

		DMTA	25 °C			55 °C		
wt-%	wt-%, TGA	E'_c/E'_r	E, MPa	σ_b, MPa	ε_b, %	E, MPa	σ_b, MPa	ε_b, %
0	0	8	131±36	17.2 ± 1.2	692 ± 93	6.3 ±1.5	3.1 ± 0.5	234 ± 41
1	0.9	-	83 ± 15	17.4 ± 1.2	700 ± 54	1.4 ± 0.2	3.2 ± 0.7	215 ± 58
2	1.7	16	119 ± 19	17.5 ± 3.9	617 ± 51	1.3 ± 0.1	3.4 ± 0.7	227 ± 57
5	4.2	36	104 ± 21	13.9 ± 2	546 ± 122	6.7 ± 0.9	2.9 ± 0.6	212 ± 57
10	9.3	24	83 ± 8	15.4 ± 1.1	574 ± 57	5.1 ± 2.2	3.2 ± 0.6	246 ± 30

b) MagSilica 50-85

		DMTA	25 °C			55 °C		
wt-%	wt-%, TGA	E'_c/E'_r	E, MPa	σ_b, MPa	ε_b, %	E, MPa	σ_b, MPa	ε_b, %
0	0	8	131±36	17.2 ± 1.2	692 ± 93	6.3 ± 1.5	3.1 ± 0.5	234 ± 41
2	2	19	103±5	15 ± 0.3	580 ± 33	1.9 ± 0.4	2.2 ± 0.3	110 ± 25
5	4.7	23	177±15	11 ± 0.2	366 ± 26	2.3 ± 0.2	1.9 ± 0.1	88 ± 11
10	9.5	31	161±9	12 ± 0.2	413 ± 18			

PDC nanocomposites - Thermal properties

PDC consist of two crystallizable segments: poly(p-dioxanone) and poly(ε-caprolactone). In the thermograms obtained from DSC four thermal transitions are observed. The glass transition $T_{g,1}$ at –53 °C is attributed to amorphous PCL-chains, $T_{g,2}$ at –14 °C is related to amorphous PPDO. $T_{m,1}$ at 39 °C corresponds to crystallites of the PCL-phase and $T_{m,2}$ at 92 °C, is attributed to the hard segment phase. Glass transition temperatures as well as melting points are not affected by incorporation of MNP (Table 2).

Table 2: Thermal properties of PDC nanocomposites with MagSilica 50-H8 (DSC)

wt-%	wt-%, TGA	$T_{m1,}$ °C	$T_{m2,}$ °C	T_{crist1}, °C	T_{crist2}, °C	T_{g1}, °C	T_{g2}, °C
0 (synthesis)	0	39.5	94	-2.2	23.4	-53.2	-13.8
0 (extrusion)	0	39.5	91.6	-0.3	17.6	-53.1	-15.4
1	0.9	41.2	92.7	5.1	19.1	-55.3	-14.5
2	1.7	40.4	92	3.1	18.3	-51.6	-14.3
5	4.2	40.3	92	1.3	18	-52.2	-15.1
10	9.3	40.6	92.8	1.5	18.5	-52.2	-15.2

The storage modulus, obtained by DMTA, identifies the PDC and its nanocomposites as a good shape-memory material because of the large drop around T_s (Figure 10). According to [30], the elasticity ratio of change in modulus between room temperature (E'_c, 25 °C), when the soft segment is partially crystalline, and 55 °C (E'_r), just above the onset of the rubbery region, is quoted for estimation the magnitude of the change in modulus as the sample undergoes shape recovery (Table 1a and b). From the fact that the drop of composites is larger than that of pure PDC, a little enhancement of the shape-memory by particle incorporation can be expected.

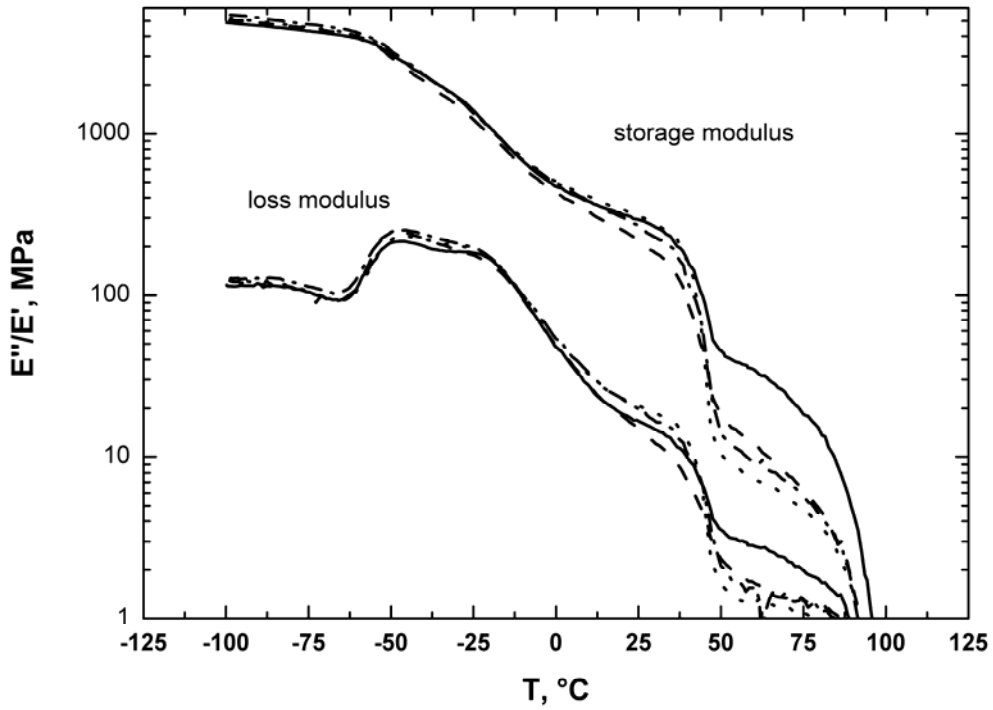

Figure 10: Storage and loss modulus (DMTA) for PDC and PDC nanocomposites with different particle (MagSilica 50-H8) content (—— 0 wt-%, — — 2 wt-%, ● ● 5 wt-%, — ● 10 wt-%).

Where no reinforcing effect by particle incorporation is observable, the storage modulus remains constant. Liu, et.al. [31] obtained an increase of storage modulus in a thermoset SMP epoxy system by incorporation of 20 wt-% SiC nanopowder with a particle dimension of 700 nm.

The peak maxima of tan δ at -49 °C and -18 °C observed in DMTA are in good agreement with DSC results (Figure 10 and Table 3). The glass transition temperatures, nonrelevant for shape-memory behavior in the case of PDC, are not affected by incorporation of nanoparticles.

Table 3: Thermal properties of PDC nanocomposites with MagSilica 50-H8 from tan δ plot (DMTA), T_g and T_m are glass transition temperatures or melting points, respectively

wt-%	wt-%, TGA	T_{g1}, °C	T_{g2} ,°C	$T_{m1,}$ °C	T_{m2}, °C
0	0	-49	-18	47.5	95.3
2	1.7	-49	-18	47.5	91
5	4.2	-49	-18	47	93
10	9.3	-49	-18	47.3	89

Mechanical properties

Consistent with DMTA results, we observed no remarkable modifications of the mechanical properties by the incorporated nanoparticles 50-H8 at 25 and 55 °C (Table 1a), except that the 50-85 nanoparticles cause a stronger decrease in elongation at break at 55 °C. The elongation at break at 25°C is only slightly decreased with growing MNP content for both particle types. The 50-H8 MNP are distinguished from the other by a hydrophobic coating with trimethyloctylsilane.

It is essential to accentuate that the mechanical properties depend strongly on the processing. The data of Table 1a and b base upon specimens that were processed on a polymer press.

Shape-Memory Properties

Shape-memory properties of the PDC composites were investigated by cyclic thermomechanical tests [15] in dependence on the programming conditions and can be quantified as customary by the shape fixity rate $R_f(N)$ and the recovery rate $R_r(N)$ [2]. From the inflection point of the strain-temperature-plot T_s can be determined. A typical three-dimensional plot for a first cycle of NC is given in Figure 11.

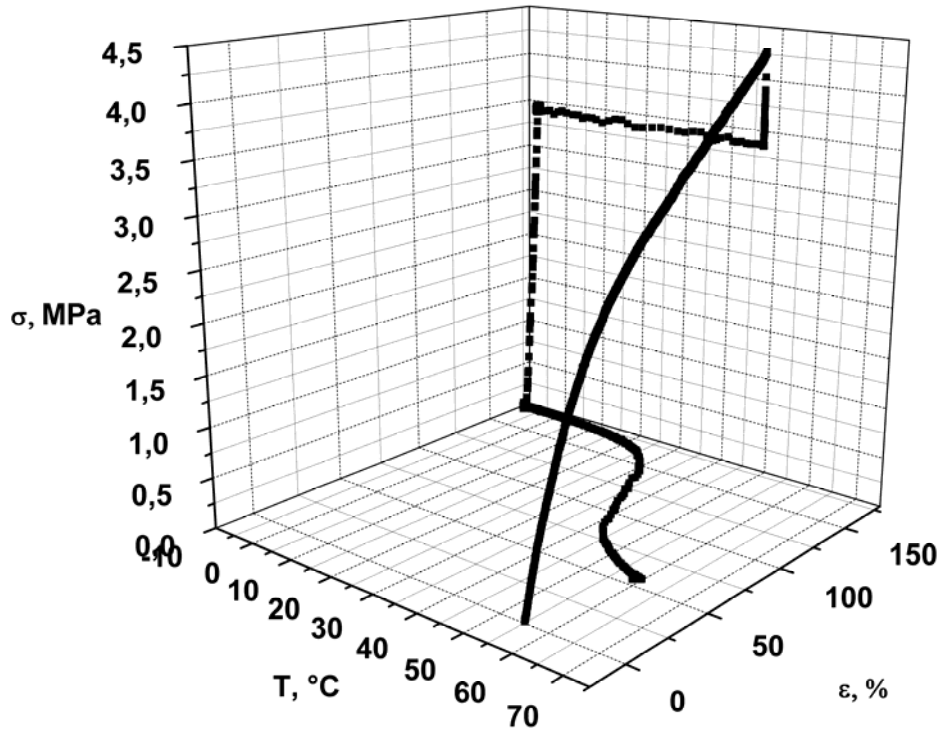

Figure 11: Cyclic thermomechanical experiment of PDC nanocomposite with 5 wt-% MagSilica50-H8, results of the first cycle are shown.

During the warm-programming (Table 4), the sample is elongated at temperature T_{high}, which is higher than T_s but lower than the thermal transition of the hard segment T_{perm}. To allow relaxation, strain is kept constant for a certain time interval. The elongated sample is now cooled for fixation of the temporary shape. This step is performed under stress control. Finally, the shape-memory effect is initiated by reheating under stress control conditions.

During the programming by cold-drawing (Table 5), the sample was elongated at T_{deform} = 25 °C, which is below the thermal transition of the switching segment T_{trans}. Fixation of the temporary shape is caused by strain-induced crystallization and strain-oriented reorganization.

Table 4: Shape-memory properties of PDC nanocomposites with MagSilica 50 H8, warm-programming

		1.cyle			2.cycle			3.cycle		
wt-%	wt-%, TGA	R_f, %	T_s,°C	R_r,%	R_f, %	T_s,°C	R_r,%	R_f, %	T_s,°C	R_r,%
0	0	90.2	51	68.2	89.4	40	92.7	91.2	39	96
2	1.7	96.9	40	66.3	97.8	39	95.9	94.9	39	97.9
5	4.2	98.7	41	77	95.2	43	97	-		

10	9.3	96.3	41	68.3	95.3	43	96.8	98.9	42.5	98.2

Table 5: Shape-memory properties of PDC nanocomposites with MagSilica 50-H8, cold-drawing

		1.cycle			2.cycle			3.cycle		
wt-%	wt-%, TGA	R_f, %	T_s,°C	R_r,%	R_f, %	T_s,°C	R_r,%	R_f, %	T_s,°C	R_r,%
0	0	82.8	45.5	54.4	90.8	39	89	90.6	39	95.9
2	1.7	80.5	43.5	73.2	90.2	38.5	95.3	90.7	38	98.1
5	4.2	83.9	45.8	57.8	94.6	39.5	93.1	94.9	39.5	97.6
10	9.3	81.9	43.5	72.4	90.4	38.5	96.1	90.7	38	98.9

All investigated PDC nanocomposites have good shape-memory properties, and for both programming procedures there is only a small influence of MNP obtainable. The recovery rates for the composites of the second and third cycle are somewhat higher than for the pure PDC, cp. DMTA results. The variations between the first and the following cycles are typical for thermoplastic SMP and caused by the material history. As a result of PCL crystallinity, the shape fixity of cold-drawn samples especially for the first cycle is remarkably lower than for warm-programmed samples where the deformation temperature is above the melting point of PCL. T_s is slightly higher for the warm-programming (second and third cycle).

4. Conclusions

Nanocomposites on the basis of biodegradable shape-memory polymers and magnetic nanoparticles are suitable for applications where a remote triggering of the shape-memory by an AC magnetic field is advantageous because the thermal, mechanical and shape-memory properties of the SMP are not decisively changed by the nanoparticles up to 10 wt-%. The latter are actually somewhat improved.

Magnetically-triggered shape-memory composites have a high application potential in medicine. Smart implants or instruments could enable surgeons to perform mechanical adjustments in a non-contact mode. Another area of applications could be on demand drug delivery from an implanted depot, which could be triggered non-invasively by a magnetic field. Especially, the PDC composite system is suitable to be further developed into a medical application, since the PDC polymer has been developed as a degradable biomaterial and T_s of the PDC materials is slightly above body temperature.

However remote triggering of PDC nanocomposites with magnetic core – shell nanoparticles in physiological environments stays a challenge. Optimization of material parameters investigated in this study might only result in maximum achievable temperatures very close

to T_s. Therefore new concepts, e.g. in the material/specimen design are required. In addition, this application area also implicates investigations regarding biocompatibility of nanocomposites and the successful realization of clinic studies. The influencing criterions on heating in an alternating magnetic field were discussed in detail. Generally the applicability of magnetically triggering has to be examined separately for any specific application.

Acknowledgement

Authors thank M. Zierke, H. Kosmella, F. Klein, and M. Schossig (GKSS, Institute of Polymer Research) for assistance with synthesis, (thermo) mechanical tests, processing PDC, and SEM, respectively. They thank also M. Lucka-Gabor (DKI, Darmstadt) for preparation of TFX nanocompounds.

Financial support from the Federal Ministry of Economics and Technology [Bundesministerium für Wirtschaft und Technologie (BMWi)] through the Federation of Industrial Cooperative Research Associations “Otto von Guericke” [Arbeitsgemeinschaft industrieller Forschungsvereinigungen “Otto von Guericke” e.V. (AiF)] (AiF-No AZ VI A2-404245/2) is gratefully acknowledged. It was a colloborative project of the DKI (Deutsches Kunststoffinstitut Darmstadt) and GKSS. Authors acknowledge Degussa Advanced Nanomaterials for providing material samples of AdNano® MagSilica.

References

[1] Lendlein A and Kelch S 2002 Shape-Memory Polymers *Angewandte Chemie International Edition* **41** 2034-57.

[2] Mohr R, Kratz K, Weigel T, Lucka-Gabor M, Moneke M and Lendlein A 2006 Initiation of shape-memory effect by inductive heating of magnetic nanoparticles in thermoplastic polymers *Proceedings of the National Academy of Sciences of the United States of America* **103** 3540-5.

[3] Buckley P R and Maitland D J 2005 Shape memory systems with integrated actuation using embedded particles *USA Patent US20050212630*.

[4] Buckley P R, McKinley G H, Wilson T S, Small W, Benett W J, Bearinger J P, McElfresh M W and Maitland D J 2006 Inductively heated shape memory polymer for the magnetic actuation of medical devices *IEEE Transactions on Biomedical Engineering* **53** 2075-83.

[5] Razzaq M Y, Anhalt M, Frormann L and Weidenfeller B 2007 Thermal, electrical and magnetic studies of magnetite filled polyurethane shape memory polymers *Materials Science and Engineering A - Structural Materials: Properties, Microstructure and Processing* **444** 227-35.

[6] Andra W and Nowak H 1998 *Magnetism in medicine* Berlin, Weinheim, New York, Chichester, Brisbane, Singapore, Toronto Wiley-VCH.

[7] Hergt R, Andra W, d'Ambly C G, Hilger I, Kaiser W, Richter U and Schmidt H-G 1998 Physical limits of hyperthermia using magnetic fine particles *IEEE Transaction on Magnetics* **34** 3745-52.

[8] Mueller-Schulte D and Schmitz-Rode T 2006 Thermosensitive magnetic polymer particles as contactless controllable drug carriers *Journal of Magnetism and Magnetic Materials* **302** 267-71.

[9] Lao L L and Ramanujan R V 2004 Magnetic and hydrogel composite materials for hyperthermia applications *Journal of Materials Science: Materials in Medicine* **15** 1061-4.

[10] Dutz S, Hergt R, Murbe J, Topfer J, Muller R, Zeisberger M, Andra W and Bellemann M E 2006 Magnetic nanoparticles for biomedical heating applications *Zeitschrift für Physikalische Chemie - International Journal of Research in Physical Chemistry & Chemical Physics* **220** 145-51.

[11] Ma M, Wu Y, Zhou J, Sun Y, Zhang Y and Gu N 2004 Size dependence of specific power absorption of Fe3O4 particles in AC magnetic field *Journal of Magnetism and Magnetic Materials* **268** 33-9.

[12] Andra W, d'Ambly C G, Hergt R, Hilger I and Kaiser W A 1999 Temperature distribution as function of time around a small spherical heat source of local magnetic hyperthermia *Journal of Magnetism and Magnetic Materials* **194** 197-203.

[13] Hergt R and Dutz S 2007 Magnetic particle hyperthermia-biophysical limitations of a visionary tumour therapy *Journal of Magnetism and Magnetic Materials* **311** 187-92.

[14] Lendlein A and Kelch S 2005 Shape-memory polymers as stimuli-sensitive implant materials *Clinical Hemorheology and Microcirculation* **32** 105-16.

[15] Lendlein A and Langer R 2002 Biodegradable, elastic shape-memory polymers for potential biomedical applications *Science* **296** 1673-6.

[16] Metcalfe A, Desfaits A C, Salazkin I, Yahia L, Sokolowski W M and Raymond J 2003 Cold hibernated elastic memory foams for endovascular interventions (vol 24, pg 491, 2003) *Biomaterials* **24** 1681.

[17] Gottfried H, Janzen C, Pridöhl M, Roth P, Trageser B and Zimmermann G 2003 Superparamagnetic oxidic paricles, processes for their production and their use Degussa AG Düsseldorf *USA Patent 6,746,767*.

[18] European *Standard EN ISO 527-2 (1996)*.

[19] Hilger I, Fruhauf K, Andra W, Hiergeist R, Hergt R and Kaiser W A 2002 Heating Potential of Iron Oxides for Therapeutic Purposes in Interventional Radiology *Academic Radiology* **9** 198-202.

[20] Chastellain M, Petri A, Gupta A, Rao K and Hofmann H 2004 Superparamagnetic silica-iron oxide nanocomposites for application in hyperthermia *Advanced Engineering Materials* **6** 235-41.

[21] Hergt R, Hiergeist R, Zeisberger M, Glockl G, Weitschies W, Ramirez L P, Hilger I and Kaiser W A 2004 Enhancement of AC-losses of magnetic nanoparticles for heating applications *Journal of Magnetism and Magnetic Materials* **280** 358-68.

[22] Jordan A, Rheinländer T, Waldofner N and Scholz R 2003 Increase of the Specific Absorption Rate (SAR) by Magnetic Fractionation of Magnetic Fluids *Journal of Nanoparticle Research* **5** 597-600.

[23] Maehara T, Konishi K, Kamimori T, Aono H, Hirazawa H, Naohara T, Nomura S, Kikkawa H, Watanabe Y and Kawachi K 2005 Selection of ferrite powder for thermal coagulation therapy with alternating magnetic field *Journal of Materials Science* **40** 135-8.

[24] Muller R, Hergt R, Zeisberger M and Gawalek W 2005 Preparation of magnetic nanoparticles with large specific loss power for heating applications *Journal of Magnetism and Magnetic Materials* **289** 13-6.

[25] Wang X, Gu H and Yang Z 2005 The heating effect of magnetic fluids in an alternating magnetic field *Journal of Magnetism and Magnetic Materials* **293** 334-40.

[26] Glockl G, Hergt R, Zeisberger M, Dutz S, Nagel S and Weitschies W 2006 The effect of field parameters, nanoparticle properties and immobilization on the specific heating power in magnetic particle hyperthermia *Journal of Physics: Condensed Matter* **18** S2935-S49.

[27] Hergt R, Dutz S, Muller R and Zeisberger M 2006 Magnetic particle hyperthermia: nanoparticle magnetism and materials development for cancer therapy *Journal of Physics-Condensed Matter* **18** S2919-S34.

[28] Brezovich I 1988 *Medical Physics Monograph* **16** 82.

[29] Pankhurst Q A, Connolly J, Jones S K and Dobson J 2003 Applications of magnetic nanoparticles in biomedicine *Journal of Physics D - Applied Physics* **36** R167-R83.

[30] Rabani G, Luftmann H and Kraft A 2006 Synthesis and characterization of two shape-memory polymers containing short aramid hard segments and poly(epsilon-caprolactone) soft segments *Polymer* **47** 4251-60.

[31] Liu Y P, Gall K, Dunn M L and McCluskey P 2004 Thermomechanics of shape memory polymer nanocomposites *Mechanics of Materials* **36** 929-40.

Appendix

Appendix A
Tecoflex® EG72D (TFX): Synthesized from methylene bis(p-cyclohexyl isocyanate) (H12 MDI), 1,4-butanediol (BD), and poly(tetramethylene glycol) (PTMG). Transition temperature at 74 °C.

Appendix B
Multiblock copolymer (PDC): Synthesized from oligo(p-dioxanone)diol, oligo(ε-caprolactone)diol and 2,2(4),4-trimethylhexanediisocyanate (TMDI), as junction unit.

Appendix C
AdNano® MagSilica 50, 50-H8 and 50-85:
Nanoscaled particles consist of an iron (II,III) oxide core in a silica matrix. The mean aggregate size (Photon correlation spectroscopy of an aqueous dispersion) is 90 nm, the mean domain size (X-ray diffraction) is 20 – 26 nm, about 25 nm, and 30-40 nm for the 50, 50-H8 and 50-85, respectively. The domain content (X-ray fluorescence analysis) is 50 - 60 wt-% (50 and 50-H8) and 85 wt-% (50-85). The 50-H8 particles have a hydrophobic shell of trimethyloctylsilane. The particles have a surface area of 40 - 65 $m^2 \cdot g^{-1}$ and a saturation magnetization of 22 - 32 $A \cdot m^2 \cdot kg^{-1}$ (50 and 50-H8) and 44-56 $A \cdot m^2 \cdot kg^{-1}$ (50-85). The density is in the range of 2.5 – 3.5 $g \cdot cm^{-3}$. All given data were provided by Degussa.

Appendix D
DSC measurements: All experiments were performed with a constant heating and cooling rate of 10 $K \cdot min^{-1}$. Whenever a maximum or minimum temperature in the testing program was reached, this temperature was kept constant for 2 minutes. The PDC samples were investigated in the temperature range from -80 °C to 150 °C. The sample was heated from 20 °C to 150 °C, then cooled down to -80 °C and again warmed up to 150 °C. All thermal transition temperatures were determined from the second heating run.

Appendix E
DMTA measurments: All experiments were performed in temperature sweep mode with a constant heating rate of 2 $K \cdot min^{-1}$. The oscillation frequency was 10 Hz. PDC samples were investigated in the temperature interval from -100 °C to 100 °C. $T_{max,\delta}$ is the maximum peak temperature of the tanδ curve.